Experimental Study and Model Predictions on Helium Release in an Enclosure with Single or Multiple Vents

Liang, Z., Barlow, K., David, R.
Canadian Nuclear Laboratories, Chalk River, Ontario, Canada
Corresponding author: zhe.liang@cnl.ca

ABSTRACT

This paper presents experiments performed at Canadian Nuclear Laboratories (CNL) to examine the dispersion behaviour of helium in a polycarbonate enclosure that was representative of a residential parking garage. The purpose was to gain a better understanding of the effect of buoyancy- or wind-driven natural ventilation on hydrogen dispersion behaviour. Although hydrogen dispersion studies have been reported extensively in the literature, gaps still exist in predictive methods for hazard analysis. Helium, a simulant for hydrogen, was injected near the centre of the floor with a flow rate ranging from 5 to 75 standard litres per minute through an upward-facing nozzle, resulting in an injection Richardson number ranging between 10^{-1} and 10^{2}. The location of the nozzle varied from the bottom of the enclosure to near the ceiling to examine the impact of the nozzle elevation on the development of a stratified layer in the upper region of the enclosure. When the injection nozzle was placed at a sufficiently low elevation, the vertical helium profile always consisted of a homogenous layer at the top overlaying a stratified layer at the bottom. To simulate outdoor environmental conditions, a fan was placed in front of each vent to examine the effect of opposing or assisting wind on the dispersion. The helium transients in the uniform layer predicted with analytical models were in good agreement with the measured transients for the tests with injection at lower elevations or with no wind. Model improvements are required for adequately predicting transients with significantly stratified profiles or with wind.

1.0 INTRODUCTION

Hydrogen energy-based vehicles or power generators are foreseen to come into widespread use in the near future. Safety information is of major importance to support the successful public acceptance of hydrogen as an energy carrier. One of the most important issues in terms of safety is the use of such hydrogen systems in confined or semi-confined areas such as garages, underground parking lots, and long tunnels. This leads to the fundamental problem of hydrogen dispersion in an enclosure, which is important for the assessment of the potential impact of combustion and the development of mitigation measures. Hydrogen mixing behaviour has been studied extensively by the nuclear industry over the past three decades. At CNL, the Large-Scale Containment Facility (LSCF) was designed and constructed to investigate hydrogen–air–steam mixing behaviour using helium as a simulant, under high-temperature and high-humidity conditions analogous to what could exist in containment during various phases of a postulated accident at a nuclear power plant. Results from those experiments formed part of a database that has been used for the validation of GOTHIC [1] [2], a general purpose thermal-hydraulics code used by the nuclear power industry for safety analysis of containment thermal-hydraulics and of hydrogen transport and mixing behaviour.

The distribution of a buoyant gas in an enclosure depends on the release rate, momentum and buoyancy fluxes, volume of the enclosure, position of the source, and ventilation conditions of the enclosure [3]. For a low-momentum release, Baines & Turner [4] and Worster & Huppert [5] showed that a stratified layer can form and move downwards from the ceiling, whereas for a highly energetic jet, the concentration can be uniformly distributed in the enclosure [6]. Between these two situations, Bolster and Linden [7] demonstrated that a vertical profile with an upper well-mixed layer followed by a stratified layer moving downwards can develop under certain release conditions. Baines & Turner [4] (whose model is referred to as “Baines’s model” hereafter) developed an asymptotic solution for the final state of the stratified layer during continuous release from small sources of turbulent buoyant plume

into a sealed enclosure. Worster & Huppert [5] ("Worster's model") further developed a time-dependent density profile during downward movement of the stratified layer front based on Baines & Turner's theory. Bolster and Linden [7] also derived a simple model that takes into account the existence of an upper well-mixed layer above the stratified layers. Prasad and Yang [8] ("Prasad's model") investigated natural and forced mixing and dispersion of hydrogen released in a partially enclosed compartment with two vents under natural and wind-assisting or wind-opposing ventilation conditions. Lowesmith et al. [9] ("Lowesmith's model") developed a mathematical model to describe the release of light gas as it mixes with air and forms a well-mixed layer of light gas/air mixture in the upper part of an enclosure with two vents.

To have a better understanding of the dispersion mechanisms and to improve the predictive methods for hydrogen risk assessment within semi-confined volumes, a series of gas dispersion experiments was performed at CNL. The first series of tests examined the helium dispersion behaviour in a 16.6 m^3 enclosure with a vent opening in the floor and distributed leaks in other places [10]. In these tests, helium was injected near the centre of the floor with an injection rate ranging from 2 to 50 SLPM (standard litres per minute[1]) through an upward-facing nozzle. During the filling process, the helium distribution predicted with Baines' and Worster's models matched the measured distributions reasonably well in this time period. After a continuous release of helium, the vertical helium profile eventually reached a steady state, which consisted of a homogenous layer at the top overlaying a stratified layer at the bottom. The helium transients in the upper uniform layer predicted with Lowesmith's and Prasad's models, assuming a vent was located in the ceiling, were in good agreement with the measured transients. The second series of tests was performed in the same enclosure with one, two or three vents on side walls. The variable parameters included injection rate, injection elevation, opposing and assisting wind speed, and vent sizes.

The first series of test results have already been reported by Liang et al. [10]. This paper presents the second series of test results. Model predictions using Lowesmith's and Prasad's models are compared with the experimental data. The findings are compared with the series 1 results and the need for model improvement are discussed.

2.0 EXPERIMENTAL METHODS

2.1 Facility

CNL's LSCF has a thick-walled concrete room with a total volume of approximately 1350 m^3. The enclosure for the experiments described here was located inside the LSCF, so the ambient conditions were stable during testing. The enclosure, shown in Fig. 1, had a total volume of approximately 16.6 m^3 (2.45 m high, 2.6 m long, and 2.6 m wide). It was constructed from engineered extruded aluminum beams and polycarbonate sheets. The polycarbonate sheets on the side walls had rubber seals along the seams. The sheets on the ceiling and floor were directly supported by horizontal beams. Silicone sealant was applied to the edges of the ceiling surface to minimize leakage. There was an entry door (2 m tall and 0.75 m wide) on the side wall with rubber seals along the seams.

In the series 1 tests [10], there was one circular vent (diameter of 5.7 cm) open in the floor surface during a test. In the series 2 tests, three openings were configured on the side walls: one upper vent (V_2) and two lower vents (V_1 and V_3). The lower vents were 10 cm above the floor and the upper vent was 20 cm below the ceiling. Each vent had a diameter of 11.4 cm. V_3 was opposite to V_1 on the same surface as V_2. There are no openings on the floor for these tests..

2.2 Measurements

The measurements consisted of helium flow rate, helium concentration, gas temperature, relative humidity (RH) and flow velocity through the opening.

[1] The standard condition is defined as a temperature of 25°C and absolute pressure of 1 atm.

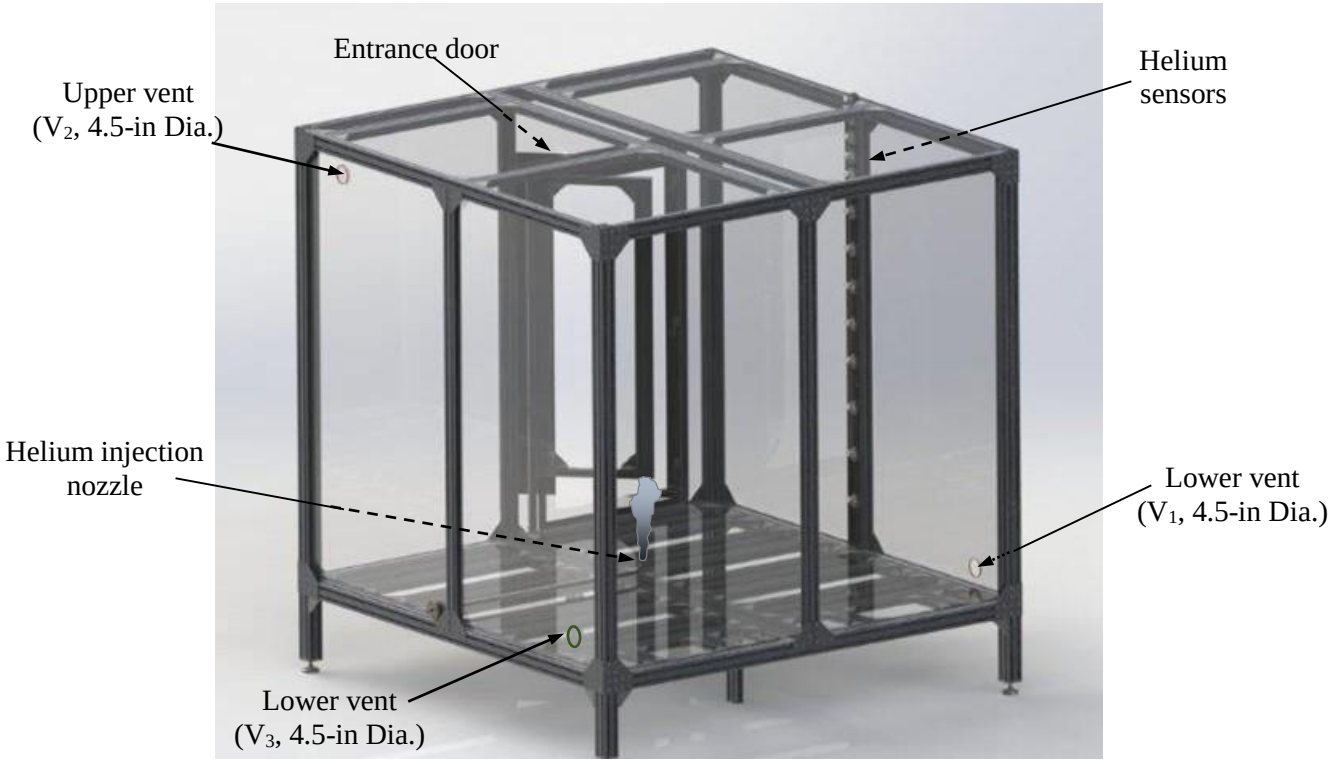

Figure 1. 3D drawing of 16.6 m^3 polycarbonate enclosure

To maintain a constant flow rate during the test, the helium injection was regulated by a flow controller (Brooks 5851E). The controller had a maximum flow of 100 SLPM and its accuracy was within ±0.5 SLPM.

The helium concentration was measured by the XEN-5320-CAN bus system. To monitor the helium spatial distribution, eighteen XEN-5320 sensors were installed in the enclosure. Sixteen sensors were mounted on the side wall at various heights. Two sensors were placed adjacent to each vent opening (V_1 or V_3, and V_2) at the same height as the centre of the opening. All the sensors were reset to zero in helium-free atmosphere and to full span in pure helium atmosphere regularly. The function of each sensor was verified using standard gases (1, 3, 5, 10, 20, and 50% helium in air). The measurement accuracy was within ±2% of reading for 3–20%[2] helium in air and within ±0.2% helium (absolute) for 1% helium in air under ambient conditions (1 atm, 20°C, and ~50% RH).

To track potential thermal stratification, the gas temperature and RH inside the enclosure were measured on the gas sample side at heights of 0.5, 1.5, and 2.4 m, using calibrated K-type thermocouples and Vaisala HMP 235 RH probes. The uncertainty of the thermocouples was ±2°C to a 95% confidence level and the uncertainty of the RH probes was approximately ±3% RH. An in-house made bi-directional flow velocity probe was mounted in the centre of each opening to measure the flow velocity through the opening. Its measurement uncertainty was approximately ±0.1 m/s.

The flow injection rate, gas temperature, relative humidity, and flow velocity were recorded by a National Instruments PXI system at a sampling rate of 1 Hz. The helium concentrations were recorded using the XEN-5320-CAN bus communication software at the same sampling rate.

2.3 Test Matrix

Six groups of tests are presented in this paper and their test conditions are as summarised in Table 1. All the tests were performed under ambient conditions (1 atm, ~20°C and ~50% RH). In each test, helium

[2] The gas concentration is always expressed on a volume basis in this paper.

was continuously injected through an upward nozzle (25 mm diameter) at a constant rate until the helium profile reached a steady or a quasi-steady state, where the increase in the maximum helium concentration was less than the measurement error (<0.2%) within half an hour. After stopping the helium injection, data were continuously collected until the helium concentration at the 2.4 m height decreased below 0.5%. In most tests, helium was injected from the bottom centre (approximately 10 cm above the floor) except in group 2, where the nozzle was elevated to a height of 0.4, 0.7, 1.0, 1.4, 1.7, or 1.9 m.

Table 1. Summary of experimental conditions

Group	Vent(s)	Injection Height (m)	Injection Rate (SLPM)	Fan	
				In front of	Speed (m/s)
1	V_1 & V_2	0.1	5, 10, 20, 30, 50, 75	-	-
2	V_1 & V_2	0.4, 0.7, 1.0, 1.4, 1.7, 1.9	10	-	-
3	V_1 & V_2	0.1	10	V_2	0.35 – 1.34
4	V_1 & V_2	0.1	10	V_1	0.65 – 1.0
5	V_2	0.1	10	-	-
6	V_1, V_2 & V_3	0.1	10	-	-

3.0 ANALYTICAL MODELS

As demonstrated in earlier studies [3]–[10], when hydrogen or helium is released into an empty enclosure filled with air, the light gas will rise as a vertical plume, reach the ceiling, spread to the sidewalls and descend in the space between the sidewalls and the plume. If the enclosure is vented through an opening close to the floor and another one close to the ceiling, the layer of buoyant fluid near the ceiling will drive a flow through the openings. Prasad and Yang [8] constructed a simple analytical model to predict natural and wind-driven mixing and dispersion of light gas in an enclosure with two vents. Fig. 2 shows a schematic diagram of Prasad's model for the pressure distribution inside and outside the compartment. The wind flow that opposes the buoyancy-induced flow is referred to as "opposing wind", while the wind flow that assists the buoyancy-induced flow is referred to as "assisting wind". As illustrated in Fig. 2 left, air enters from the lower vent and hydrogen-air mixture exits from the upper vent for cases with small opposing wind, assisting wind or no wind, while the flow is reversed with large opposing wind as shown in Fig. 2b.

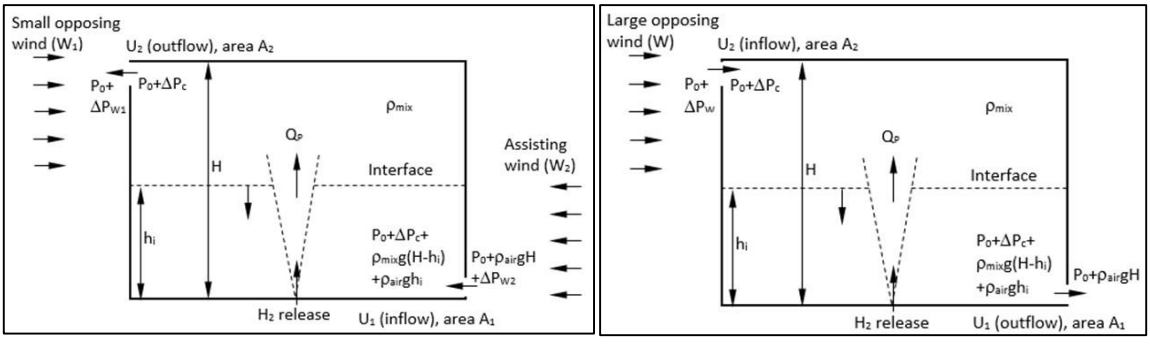

Figure 2. Schematic diagram of the pressure distribution across vents in case with no wind, or with small opposing or assisting wind (left), and with large opposing wind (right)

In Prasad's model, the gas mixture in the upper region is assumed to be well mixed and the lower region is just ambient air, except in the region surrounding the plume. The velocity U_j through the vent j

(subscript "1" for inflow and "2" for outflow) and the wind velocity are related to the pressure difference, ΔP_j, using Bernoulli's theorem, assuming no loss at the vent,

$$U_j = \sqrt{\frac{2\Delta P_j}{\rho}}, \tag{1}$$

where ρ corresponds to the density of the upstream gas mixture.

The volumetric flow rate, Q_j, through the vent j is related to the velocity U_j according to:

$$Q_j = C_{dj} A_j U_j, \tag{2}$$

where C_{dj} is the discharge coefficient (a value of 0.6 was used for the predictions of this paper) and A_j is the cross-sectional area of vent j.

The location of the instantaneous interface (h_i) is obtained by the conservation of total volume of the upper layer:

$$\frac{d[(H-h_i)S]}{dt} = Q_P - C_{d2} A_2 U_2, \text{ then } \frac{dh_i}{dt} = \frac{C_{d2} A_2 U_2 - Q_P}{S}, \tag{3}$$

where H and S are the height and cross-sectional area of the compartment, and Q_p is the volumetric flow rate of hydrogen-air mixture through the plume region across the interface, which is solved using the classical plume mixing model presented by Prasad and Yang [8].

The accumulation of hydrogen in the compartment is dependent on the hydrogen release rate, Q_{H2}, and the outflow, taking into account Equation (3),

$$\frac{d[(\rho_{mix} Y_{H2})(H-h_i)S]}{dt} = \rho_{H2} Q_{H2} - \rho_{mix} Y_{H2} (C_{d2} A_2 U_2), \text{ then } \frac{d[\rho_{mix} Y_{H2}]}{dt} = \frac{\rho_{H2} Q_{H2} - \rho_{mix} Y_{H2} Q_P}{(H-h_i)S}, \tag{4}$$

where ρ_{H2} is the density of pure hydrogen, ρ_{mix} is the density of the upper layer mixture, and Y_{H2} is the mass fraction of hydrogen in the upper layer.

Assuming that the flow is incompressible, the inflow and outflow rates are balanced with the hydrogen release,

$$Q_{H2} = \sum Q_j, \tag{5}$$

where Q_j is positive for inflow and negative for outflow.

The ordinary differential Equations (3) and (4) are solved together to obtain the location of the interface and the density of the upper layer, then the mass fraction of hydrogen as a function of time.

Lowesmith's model is similar to Prasad's model such that light gas-air mixture is accumulated in the upper region. Additional parameters are considered in Lowesmith's model, such as elevation of the hydrogen jet and elevation of the outflow vent. Its model equations are not repeated in this paper.

4.0 RESULTS AND DISCUSSION

4.1 Experimental Measurements

4.1.1 Group 1: Two Vents, Bottom Injection, No Wind

The time transients of helium concentrations and vent velocities of a selected group 1 test are shown in Fig. 3. The vertical helium profiles during and after the injection of this test are shown in Fig. 4. The injection rate of this test was 10 SLPM. Note that the raw signals of the helium concentration and velocity measurements were smoothed using Origin's Fast Fourier Transform Filter with a 100-point window. The smoothed traces are shown in the figures.

Shortly after the start of helium injection, the increase in the helium concentration at a height of 2.4 m was detected. The helium concentrations at lower elevations also started increasing gradually as the helium layer moved downward. The helium concentrations at all elevations increased essentially linearly

at the beginning. After the helium was injected for about 2 h, the variation in the helium concentrations at all elevations was small, suggesting the helium distribution approached a steady (or quasi-steady) state. The centre of the upper vent (V_2) was at 2.25 m height and the helium concentration at V_2 was identical with that measured at 1.6 m height and above (i.e., the curves overlapped). The centre of the lower vent (V_1) was at 0.1 m height and the helium concentration at V_1 was identical with that measured at 0.25 m height, suggesting that the helium was also well mixed at 0.25 m height and below.

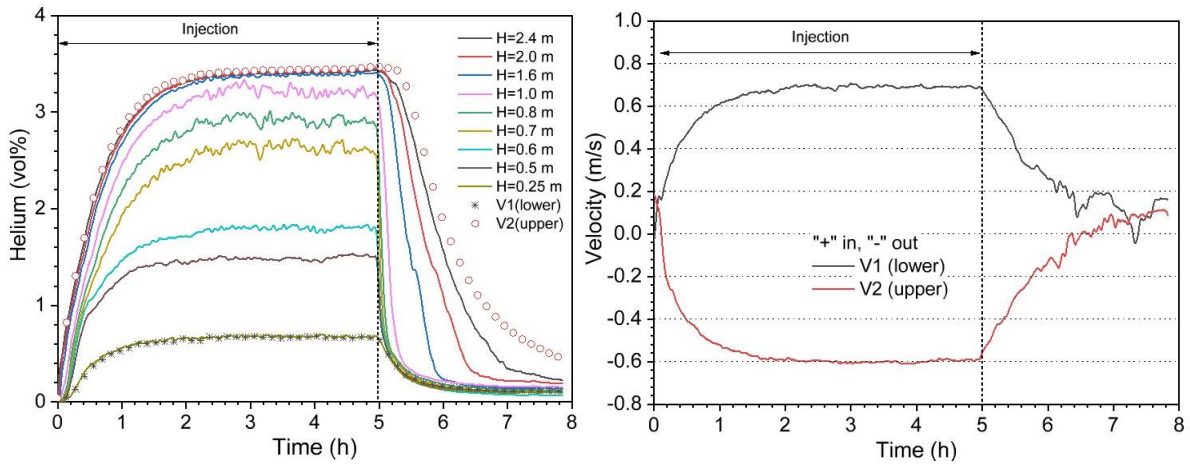

Figure 3. Time transients of helium concentrations along height (left) and vent flow velocities (right) for injection rate of 10 SLPM group 1 tests (two vents, bottom injection, no wind)

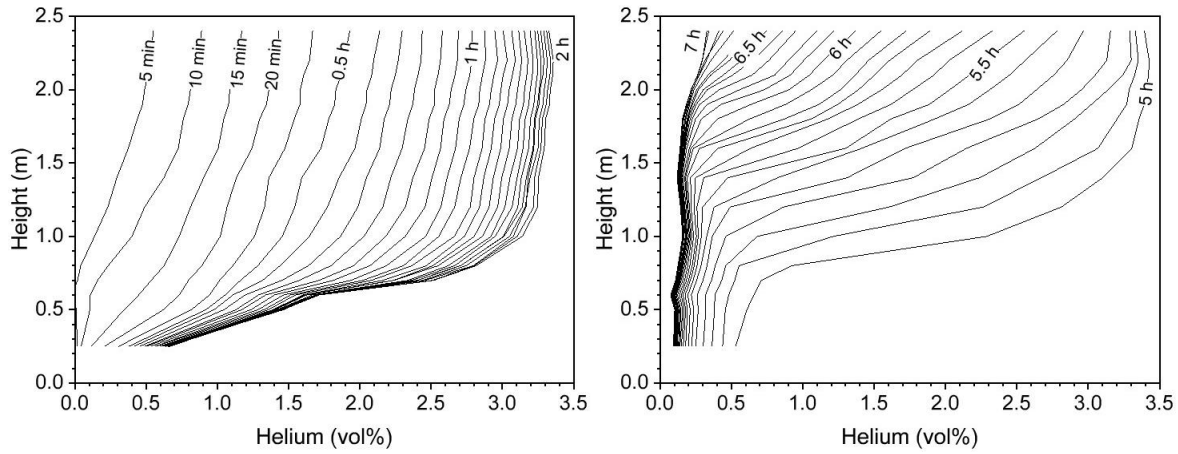

Figure 4. Vertical helium profiles during (left) and after (right) helium injection for injection rate of 10 SLPM of group 1 tests (two vents, bottom injection, no wind)

As labeled on the velocity plot in Fig. 3 (right), the positive sign stands for “flow in” and the negative one for “flow out”. At time zero, there was a weak flow (~0.2 m/s) across each vent representing the background flow induced by the building ventilation. As soon as the helium injection started, both flow velocities (absolute values) started increasing and the flow direction reversed with air entering from the lower vent (V_1) and helium-air mixture exiting from the upper vent (V_2). Similar to the helium concentrations transients, both flow velocities increased quickly at the beginning, and then gradually approached a steady state. In theory, the magnitude of the velocity at V_2 should be higher than that at V_1 because the total exit flow was higher than the inflow and the mixture density was lower at V_2, but the measured velocity at V_2 was slightly smaller than that at V_1, indicating that helium-air mixture must have exited from the distributed leaks in the upper region, as observed previously [10].

After the helium injection stopped, the helium concentrations at all elevations started decreasing immediately. The helium in the upper well-mixed layer (>1.0 m height) became stratified, whereas the lower stratified layer was quickly mixed. The decay rate was slower at higher elevations, particularly above 2 m height. The flow velocity at each vent also started to decrease as soon as the helium injection

stopped. At the end of the test, the flow velocity at each vent approached zero, but the helium concentration at the upper vent (V_2) was always slightly higher than that at 2.4 m height, suggesting the residual helium accumulated in the vicinity of the upper vent.

4.1.2 Group 2: Two Vents, Elevated Injection, No Wind

The vertical helium profiles of two group 2 tests are shown in Fig. 5 to demonstrate the effect of injection height. Elevating the injection from 0.1 to 1.0 m (Fig. 5 left), the helium remained relatively well mixed above 1.6 m height, but the helium concentration started to decrease significantly below 1.4 m height. A sharp concentration gradient appeared between 1.2 m and 1.5 m heights. The helium concentration was negligibly small (<0.2%) below 1.0 m height. Further increasing the injection height to 1.70 m (Fig. 5 right), the helium became highly stratified above 1.8 m height. Helium was not detected below 1.6 m height. This trend is consistent with the correlation developed by Cleaver et al. [11], which shows that a relatively uniform ceiling layer can form when the distance between the release elevation and the ceiling, Z_r, is large in comparison to the characteristic dimension of the ceiling, such that:

$$Z_r > 0.38\sqrt{A_C} = 1.0\ m, \tag{6}$$

where A_c is the area of the ceiling, which is 6.76 m^2 for the present enclosure.

When the injection was at 1.7 m height, the distance between the exit of the injection and the ceiling was close or less than 1.0 m, so a well-mixed ceiling layer was not able to be developed.

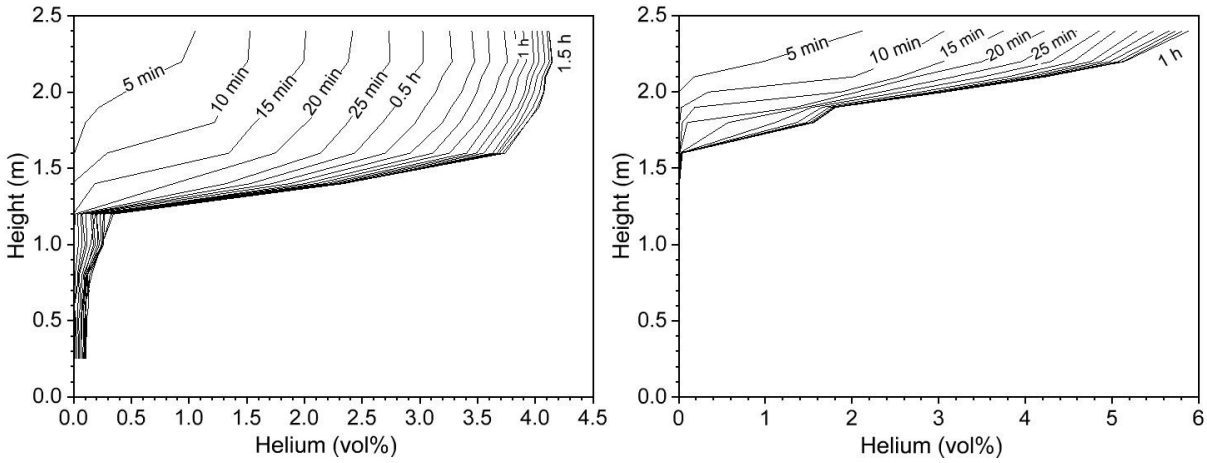

Figure 5. Vertical helium profiles for injection heights at 1.0 m (left) and 1.7 m (right) with 10 SLPM injection rate of group 2 tests (two vents, elevated injection, no wind)

4.1.3 Groups 3 & 4 Tests (Two Vents, Bottom Injection and with Wind)

For tests in groups 3 and 4, a 30-cm diameter Dyson fan was placed in front of either the upper vent (V_2) or lower vent (V_1) at a distance of 71 cm. The central axis of the fan's aperture (opening) was aligned with that of the corresponding vent. The fan always blew toward the vent. The fan velocity measured in the centre of the top vent varied from 0.35 to 1.35 m/s. At a given vertical plane in the downstream flow, the velocity decreased linearly from the top to the bottom of the fan. The time transients of helium concentrations and vent velocities of two group 3 (opposing wind) tests and one group 4 (assisting wind) test are shown in Figs. 6 to 8.

With an opposing wind speed of approximately 0.61 m/s (Fig. 6), the general trends of the helium concentration and velocity transients were the same as the group 1 tests except that the maximum helium concentration was higher. The vent flow direction reversed at ~0.85 h. The velocity at V_1 was maintained relatively steady at ~0.41 m/s, but the velocity at V_2 became negative between 0.85 and 3 h, and oscillated around zero after 3 h. Further increasing the wind speed to approximately 1.3 m/s (Fig. 7), the fan-induced flow was always dominant ("in" from V_2 and "out" from V_1). The difference in the helium

concentration between the ceiling and the floor was less than 1% and a steady state was never reached before the helium injection stopped at 3 h.

With assisting wind (Fig. 8), the helium distribution and flow pattern were similar to the small opposing wind test (Fig. 6) and the test with no wind (Fig. 4). Prior to helium injection, the fan-driven flow was already established. The flow velocity at the lower vent was approximately 1.0 m/s.

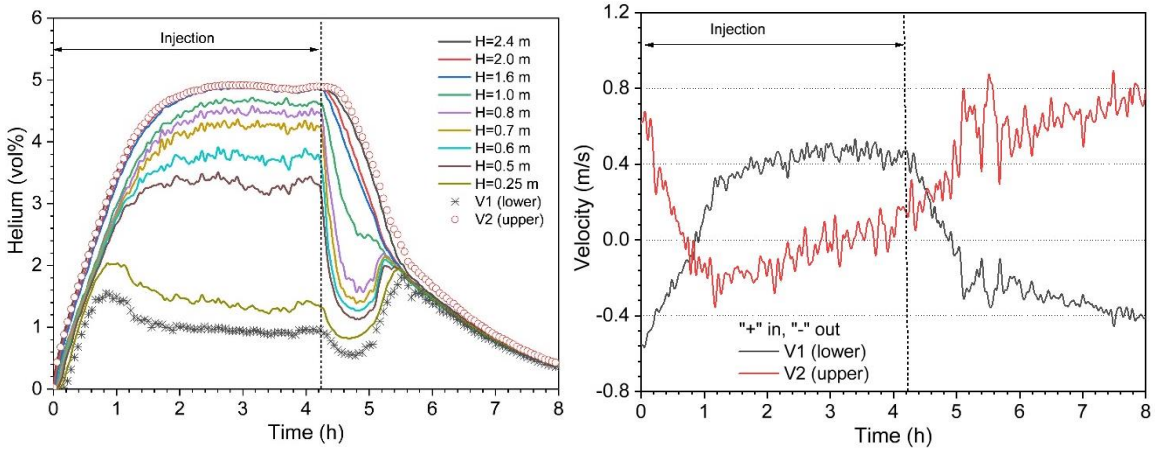

Figure 6. Time transients of helium concentrations along height (left) and vent flow velocities (right) for injection rate of 10 SLPM of group 3 tests (two vents, bottom injection, 0.6 m/s opposing wind)

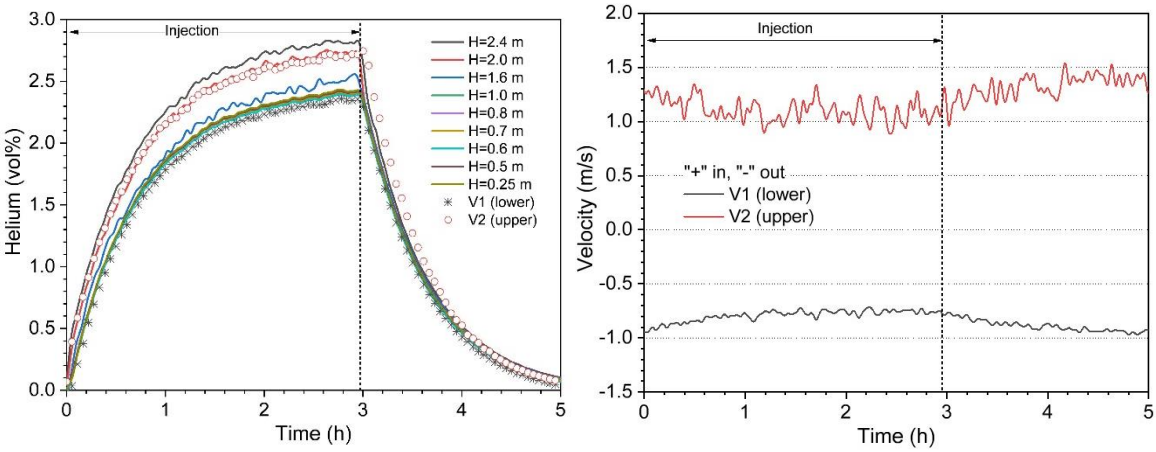

Figure 7. Time transients of helium concentrations along height (left) and vent flow velocities (right) for injection rate of 10 SLPM of group 3 tests (two vents, bottom injection, 1.3 m/s opposing wind)

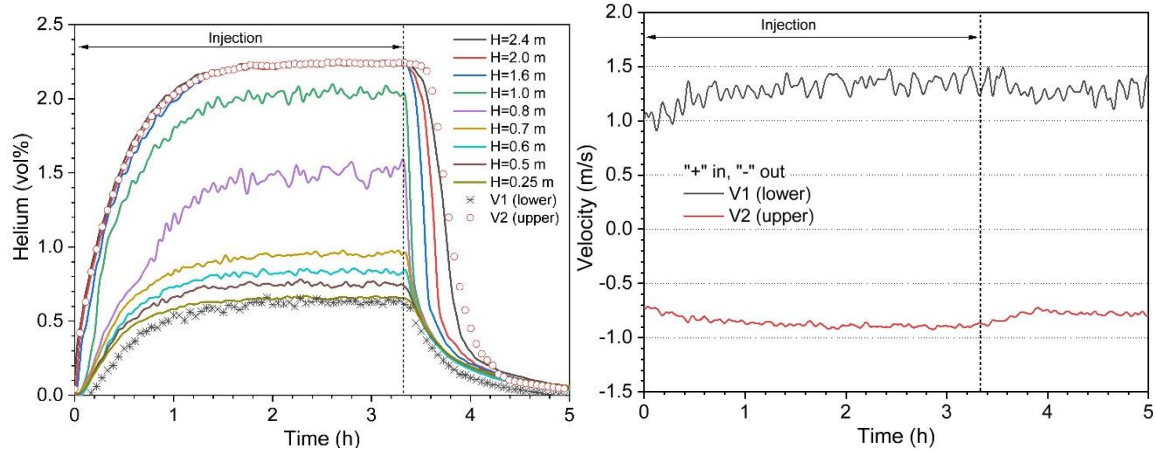

Figure 8. Time transients of helium concentrations along height (left) and vent flow velocities (right) for injection rate of 10 SLPM of group 4 tests (two vents, bottom injection, 1.3 m/s assisting wind)

4.1.4 Groups 5 & 6: One or Three Vents, Bottom Injection, No Wind

To examine the sensitivity of different sizes between the upper and lower vents, the lower vent V_1 was temporarily blocked in group 5 tests and both V_1 and V_3 were open in group 6 tests. The other parameters remained the same as in the group 1 tests. The time transients of helium concentrations and vent velocities of one group 5 test and one group 6 test are shown in Figs. 9 and 10, respectively.

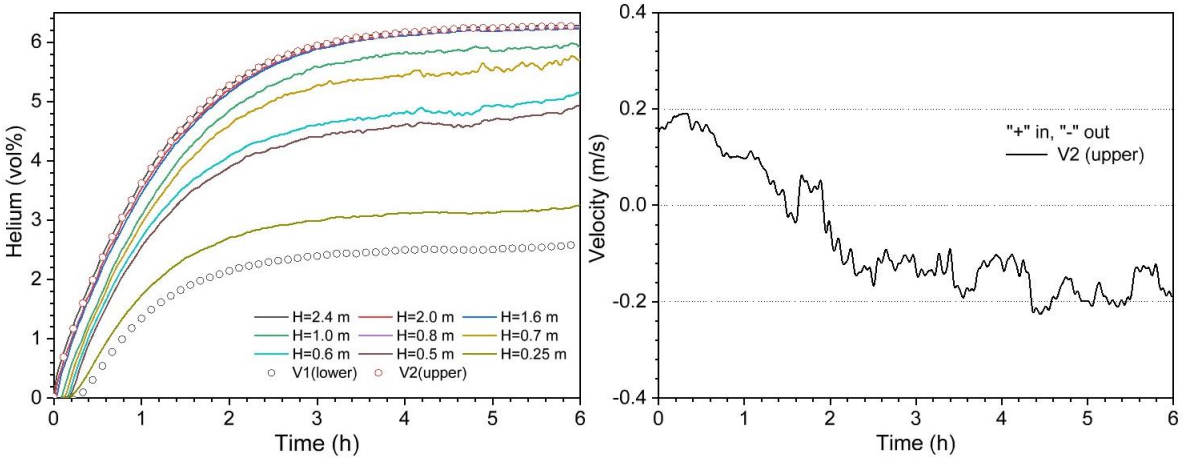

Figure 9. Time transients of helium concentrations along height (left) and vent flow velocities (right) for injection rate of 10 SLPM of group 5 tests (one vent, bottom injection, no wind)

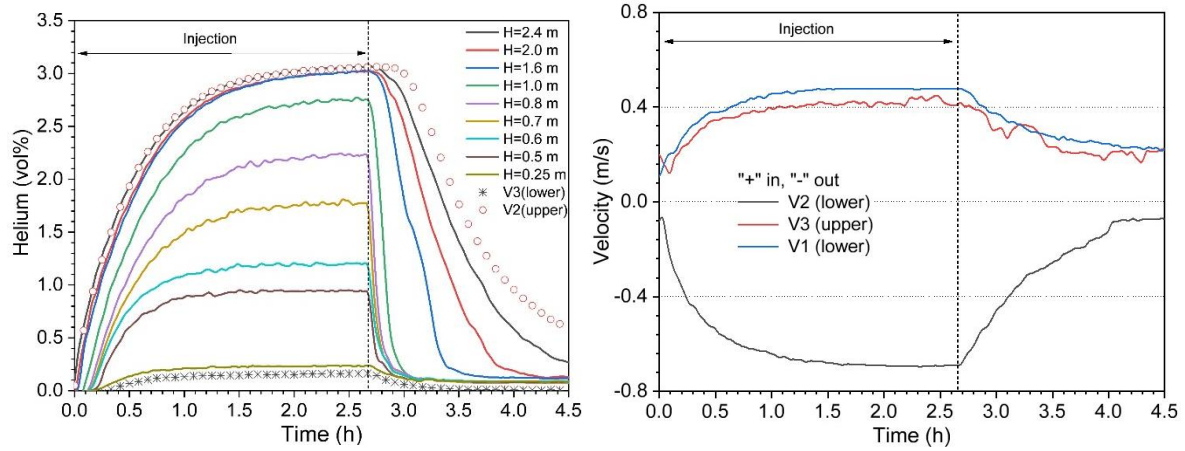

Figure 10. Time transients of helium concentrations along height (left) and vent flow velocities (right) for injection rate of 10 SLPM of group 6 tests (three vents, bottom injection, no wind)

The structure of the helium profiles of the group 5 test (Fig. 9) remained the same as the group 1 test, but the helium concentrations at all elevations were significantly higher and the flow velocity at the upper vent was significantly smaller. This suggests that air entered from distributed leaks in the lower region, but the total amount of outflow from the upper vent was restricted by the air ingress rate in the lower region, which was much smaller than that with the lower vent V_1 open. Therefore, the amount of leakage in the lower region was the limiting factor for the overall buoyancy-driven flow.

In group 6 with two lower vents open (Fig. 10), the helium concentrations at all elevations were slightly lower than in the group 1 test. The velocities at the two lower vents (V_1 and V_3) were approximately the same and their values were slightly larger than half of the value recorded at V_1 in the group 1 test. The absolute velocity at the upper vent V_2 was also slightly larger. In this case, the upper vent was the limiting factor for the buoyancy-driven flow.

4.2 Model Predictions

Prasad's and Lowesmith's model predictions are compared with the time transients of measured helium concentration at 2.4 m height (well-mixed layer) for the group 1 tests in Fig. 11. As discussed earlier, the measured flow velocity at the upper vent was smaller than that at the lower vent, suggesting that a certain amount of helium-air mixture exited through distributed leaks in the upper region. For each test, the actual vent size (11.4 cm diameter) and an estimated vent size (12.7 cm) were used in the predictions. Prasad's model predictions with both vents of 11.4 cm matched the measurements of all the tests very well, while the measurements were slightly under-predicted with both vents of 12.7 cm. Lowesmith's model predictions with both vents of 12.7 cm matched the measurements of all the tests very well, but the measurements were over-predicted with both vents of 11.4 cm. At a given injection rate, the maximum helium concentration decreased with an increase in either vent size. The variation was more significant at higher flow rates. Overall, Lowesmith's model predictions with both vents of 12.7 cm might be more reliable considering that distributed leaks did exist in the upper region.

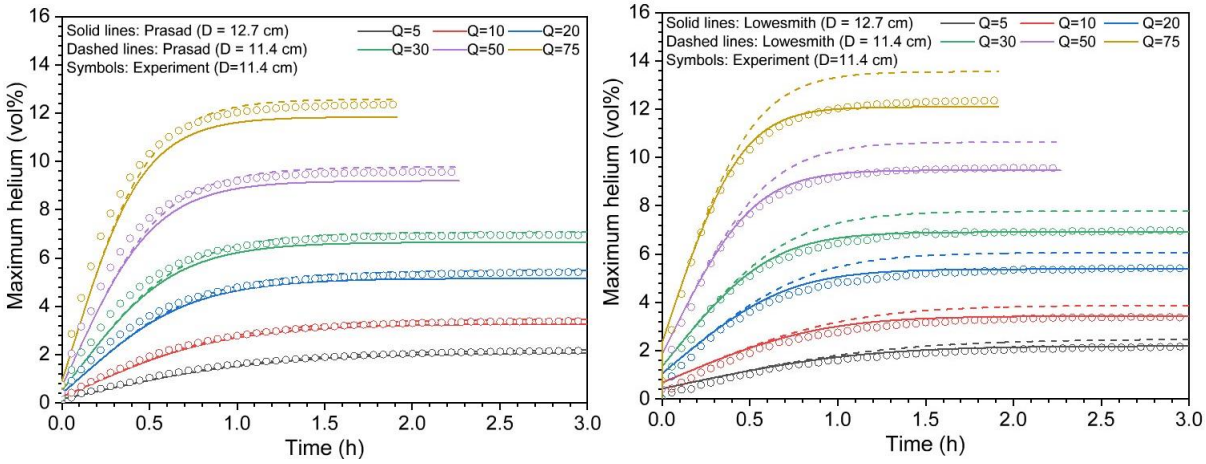

Figure 11. Comparison of helium concentration in the well-mixed layer with predictions of Prasad's model (left) and Lowesmith's model (right) for group 1 tests (two vents, bottom injection, no wind)

Model predictions for other groups of tests are not presented in this paper for several reasons. First, the injection height was not a variable in Prasad's model. Second, Lowesmith's model is not applicable for opposing wind and Prasad's model had issues with convergence of the solutions for a wind speed greater than 0.5 m/s. Third, the sizes of both vents were assumed to be the same in Lowesmith's model.

4.3 Steady States

Fig. 12 compares the steady-state model predictions with the helium concentration measured at 2.4 m height, the total volume of helium and vent velocities as a function of injection rate for the group 1 tests. The dashed lines have been added to show the trend of the measured data. In both models, the total volume of helium was calculated by multiplying the helium concentration in the upper well-mixed layer and the volume of the upper layer. In the experiments, the total volume of helium was determined by integrating the vertical helium concentration recorded at each sensor with a trapezoidal rule. The maximum helium concentration, flow velocity (absolute value) at each vent and total volume of helium increased with an increase in the injection rate. At a given inject rate, Prasad's model tended to predict a slightly smaller helium concentration, higher vent flow velocities, and lower elevation of the interface (thicker upper layer) than Lowesmith's model. The total volume of helium predicted by both models was approximately the same with the same vent sizes. Overall, Lowesmith's model predictions matched the measured data relatively well when an effective 12.7 cm vent diameter was applied.

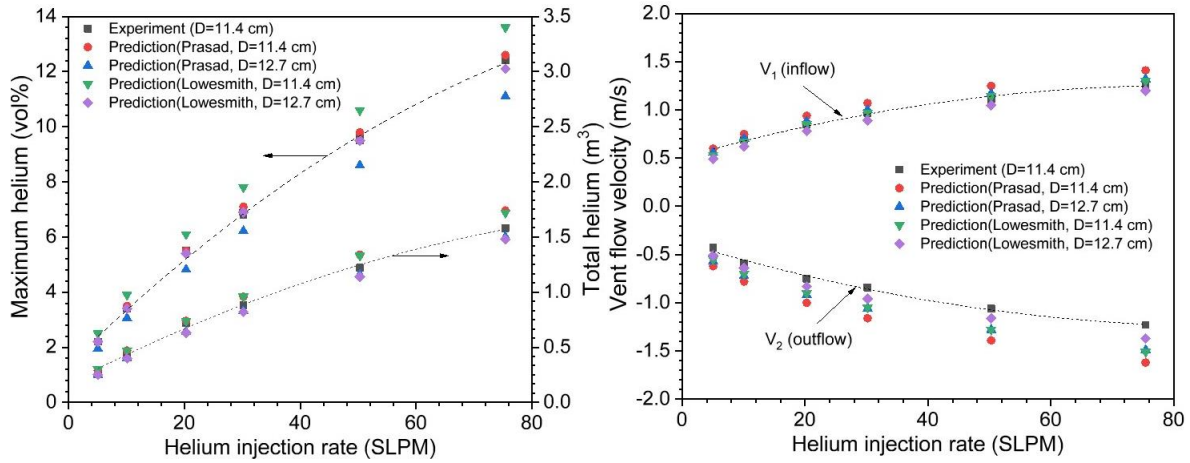

Figure 12. Comparison of steady-state maximum helium concentration and total helium in the well-mixed layer (left) and vent flow velocities (right) as a function of helium injection rate

The measured steady-state helium concentration at 2.4 m height and total volume of helium are shown as a function of injection height for the group 2 tests in Fig. 13 and as a function of wind speed for the group 3 tests in Fig. 14. When the injection was at 1 m height and lower, the maximum helium concentration increased essentially linearly with an increase in the injection height. In these tests, the vertical helium profile still consisted of an upper uniform layer and a stratified lower layer. When the injection was elevated above 1 m height, the maximum helium concentration increased significantly with an increase in the injection height. In these tests, the upper well-mixed layer was very thin or disappeared due to the small distance between the ceiling and the injection to form an upper layer. The total volume of helium decreased linearly with an increase in the injection height.

When the opposing fan speed was less than 0.8 m/s, the maximum helium concentration increased with an increase in the wind speed. In this flow range, the buoyancy-driven flow was dominant, so the flow pattern remained the same as shown in Fig. 2 (left). Further increasing the fan speed, the fan-driven flow was dominant and the flow was reversed as shown in Fig. 2 (right). The maximum helium concentration decreased with an increase in the fan speed. The trend was the same as the assisting wind except the helium concentration was well mixed with large opposing wind. The total helium always followed the same trend as the maximum helium concentration for the group 3 and 4 tests.

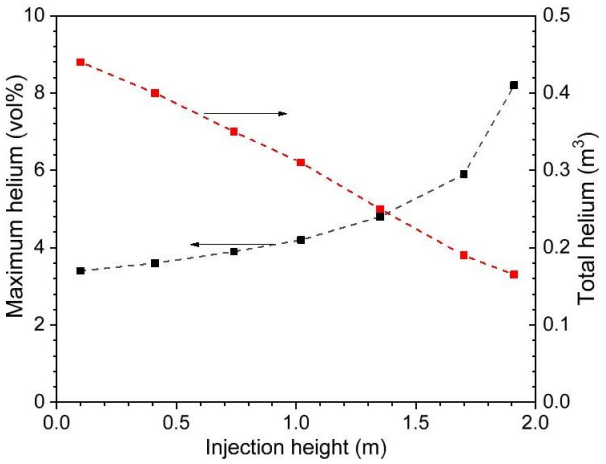

Figure 13. Steady-state maximum helium concentration and total helium in the well-mixed layer as a function of injection height

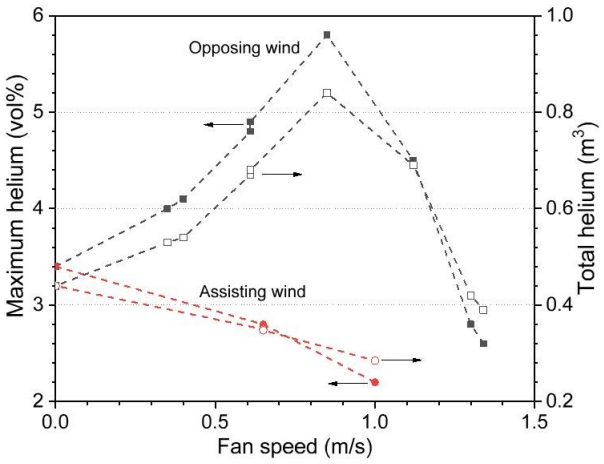

Figure 14. Steady-state maximum helium concentration and total helium in the well-mixed layer as a function of fan speed

5.0 CONCLUSIONS

This study examined the helium, a simulant for hydrogen, dispersion behaviour in a 16.6 m^3 enclosure with single or multiple vents. Helium was continuously released from an upward-facing nozzle until a

steady-state was reached. The effect of various parameters on the helium distribution was investigated, including helium injection rate and elevation, opposing and assisting wind speed, and vent sizes.

With no wind, the helium profile always consisted of a well-mixed upper layer and a stratified lower layer when the distance between the ceiling and the injection nozzle was greater than a critical value, which is related to the square root of the cross-sectional area of the enclosure. When the distance was too small, the uniform layer disappeared and the helium was linearly stratified above the injection nozzle. The stratification was greater with the injection at a higher elevation. The maximum steady-state helium concentration was larger at a higher injection rate or with a smaller vent size. With assisting or small opposing wind, the helium profile was the same as that with no wind. With large opposing wind, the flow was dominated by the wind and helium was nearly well mixed in the entire enclosure. The maximum helium concentration increased with an increase in the small opposing wind speed, but the trend was opposite with large opposing or assisting wind. The predictions using Prasad's and Lowesmith's models agreed reasonably well with the experimental data when the helium was released at lower elevations with no wind. Any discrepancy was partially attributed to the unknown distributed leaks in the upper region of the enclosure. Further model development is required for the analysis of the tests with significantly stratified profile or with wind that are not presented in this paper.

The size and shape of the enclosure are considered representative of residential parking garages, so the experimental data should be useful for validation of hydrogen analysis codes and models in such situations.

ACKNOWLEDGEMENT

The authors gratefully acknowledge the financial support from Atomic Energy of Canada Limited, under the auspices of the Federal Nuclear Science and Technology Program.

REFERENCES

1. Voelsing, K., GOTHIC - Thermal Hydraulic Analysis Package Technical Manual Version 8.2 (QA), Electric Power Research Institute Inc., 2016 October.
2. Liang, Z. and Chin, Y-S., Simulation of Buoyancy Induced Gas Mixing Tests Performed in a Large Scale Containment Facility Using GOTHIC Code, Proceedings of 19th Pacific Basin Nuclear Conference (PBNC), 2014 August 24–28, Vancouver, BC, Canada.
3. Cariteau, B., Brinster, J., and Tkatschenko, I., Experiments on the Distribution of Concentration due to Buoyant Gas Low Flow Rate Release in an Enclosure, *Int J Hydrog Energy*, **36**, 2011, pp. 2505-2512.
4. Baines, W.D. and Turner, J.S., Turbulent Buoyant Convection from a Source in a Confined Region, *J Fluid Mech*, **37**, Part 1, 1969, pp. 51–80.
5. Worster, M.G. and Huppert, H.E., Time-Dependent Density Profiles in a Filling Box, *J Fluid Mech*, **132**, 1983, pp. 457–466.
6. Cariteau, B. and Tkatschenko, I., Experimental Study of the Concentration Build-Up Regimes in an Enclosure without Ventilation, *Int J Hydrog Energy*, **37**, 2012, pp. 17400–17408.
7. Bolster, D.T. and Linden, P.F., Containments in Ventilated Filling Boxes, *J Fluid Mech*, **591**, 2007, pp. 97–116.
8. Prasad, K. and Yang, J.C., Vertical Release of Hydrogen in Partially Enclosed Compartment: Role of Wind and Buoyancy, *Int J Hydrogen Energy*, 36, 2011, pp. 1094-1106.
9. Lowesmith, B., Hankinson, G., Spataru, C., and Stobbart, M., Gas Build-Up in a Domestic Property Following Releases of Methane/Hydrogen Mixtures, *Int J Hydrogen Energy*, 34 (14), 2009, pp. 5932–5939.
10. Liang, Z., McKenna, A., Clouthier, T., and David. R., Experimental Study on Accumulation of Helium Released into a Semi-Confined Enclosure with Distributed Leaks, in press, *Int J Hydrog Energy*, 2020
11. Cleaver, R.P., Marshall, M.R., and Linden, P.F., The Build-Up of Concentration within a Single Enclosed Volume Following a Release of Natural Gas, *J Hazard Mater*, 36, 1994, pp. 209–226.